Applied Surface Science 515 (2020) 146062

Contents lists available at ScienceDirect

Applied Surface Science

journal homepage: www.elsevier.com/locate/apsusc

Full Length Article

Porous Cu_xO/Ag_2O (x = 1, 2) nanowires anodized on nanoporous Cu-Ag bimetal network as a self-supported flexible electrode for glucose sensing

Qian Zhang[1], Man Li[1], Zhifeng Wang, Chunling Qin*, Mengmeng Zhang, Yongyan Li*

School of Materials Science and Engineering, Hebei University of Technology, Tianjin 300130, China

ARTICLE INFO

Keywords:
Nanoporous
Dealloying
Anodizing
Glucose sensor
Flexibility

ABSTRACT

At present, it is of great significance to develop novel free-standing electrode materials with high porosity and excellent glucose electrocatalytic performance for glucose detection. Herein, we synthesize two types of self-supported electrodes with Cu_xO or Cu_xO/Ag_2O (x = 1, 2) nanowires grown on the nanoporous substrate via dealloying of $Cu_{50-x}Zr_{50}Ag_x$ (x = 0 and 7.5 at%) metallic glasses, followed by anodizing and calcination. The effects of adding Ag element into $Cu_{50}Zr_{50}$ MG precursor on the morphology and electrochemical performance of electrodes are systematically investigated. Compared with cluster-like copper monometallic oxide nanowire on nanoporous Cu (Cu_xO@NPC, x = 1, 2) electrode, the in-situ grown copper-silver bimetallic oxide nanowire on nanoporous Cu-Ag (Cu_xO/Ag_2O@NP-CuAg) electrode with tip convergence and hierarchical porous structure possesses better electrooxidation performance for glucose. The newly developed Cu_xO/Ag_2O@NP-CuAg electrode exhibits a high sensitivity of 1.31 mA mM^{-1} cm^{-2} and wide linear range up to 15 mM, outstanding anti-interference ability and stability. The enhanced electrocatalytic performance is mainly due to the synergistic effect of Cu and Ag elements as well as unique structural characteristics. Meanwhile, the possible glucose electrocatalytic mechanism of Cu_xO/Ag_2O@NP-CuAg electrode is proposed. The as-developed materials with good glucose sensing performance and flexibility will be highly promising in wearable glucose sensors.

1. Introduction

Rapid and precise monitoring of glucose value is vital in the clinical diagnosis, food industry and biotechnology [1–3]. As reported, electrochemical detection for glucose is the most popular and effective technique because of its comprehensive superiority of fast, accurate, low cost and ease of use [4–6]. Therefore, the electrode material is considered as the key component of glucose sensors.

In previous research, transition metals (Cu, Ni, Co, Ag, etc.) have been widely studied owing to their remarkable conductivity, effective catalytic activity and abundant reserve [7–10]. However, they are easily corroded in solution, passivated in the air and affected by interference, which result in reduced accuracy and poor selectivity. It has been reported that sensing performance of electrode materials was improved via preparing transition metal composites and micro-nanostructured materials [11]. Meanwhile, the composites with one or more electrochemical active elements could produce a unique synergistic effect, which may further improve electrocatalytic performance of electrode as compared to pure metal materials [12–15]. On the other hand, micro-nanostructured (e.g. nanowires, nanotubes, nanospheres and nanoflowers, etc.) [16–20] increase the specific surface area so as to provide more reactive sites and reduce the ion diffusion path. Based on above design strategy, a great variety of materials so far has been exploited, such as NiO/Ag nanofibers [21], CuO nanoparticles/carbon nanotube [22], and Cu_2O nanocubes wrapped by graphene nanosheets [23] and so on.

More recently, bimetal Cu-Ag or oxides nanocomposites have especially attracted widespread attention in glucose sensors, due to the presence of $Cu^{3+}/Cu^{2+}/Cu^{+}$ redox couple as well as wonderful electrocatalytic and conductivity performance of Ag element [24–26]. Cu-Ag nanocomposites with low Ag constructed by Xu and his co-workers [27] exhibited better electrocatalytic activity compared to pure Cu nanomaterials fabricated with the same procedure. Zhang et al. [28] reported that the electrode modified by Cu-Ag_2O nanowalls displayed higher catalysis for glucose oxidation than traditional Ag_2O nanoflowers. Regrettably, these electroactive materials require to be loaded onto the substrate materials (i.e. glassy carbon electrode, Ni foam, and ITO glass, etc.) with the help of polymer binder. It not only seriously increases electronic transfer resistance, leading to reduce conductivity, but also slowly cut down long-term stability because of uncontrollable

* Corresponding authors.
E-mail addresses: clqin@hebut.edu.cn (C. Qin), liyongyan@126.com (Y. Li).
[1] These authors contributed to this work equally.

https://doi.org/10.1016/j.apsusc.2020.146062
Received 16 January 2020; Received in revised form 4 March 2020; Accepted 11 March 2020
Available online 12 March 2020
0169-4332/

agglomerating or shedding of the active substance. Furthermore, complex and time-consuming preparation processes further limit their practical application. In order to solve these issues, developing free-standing electrode materials without binder has been becoming a research hotspot.

It is worth noting that anodizing is an effective method to obtain binder-free and self-standing electrode composites by sacrificing portion of the substrate material [29]. Up to now, based on various conductive substrates, such as metal foil, foamed metal or nanoporous matrix, the self-supporting electrode with diversified nanowire morphologies for glucose oxidation has been developed by anodization technology [24,30,31]. It has been demonstrated that nanoporous substrate with high specific surface area and good conductivity exhibits more distinct structural features as well as size effects, which is beneficial to ion diffusion and electronic transfer [2]. In addition, anodizing, namely in-situ growth on the substrate, is able to effectively integrate the superior electrical conductivity and skeleton supporting of the matrix, which contributes to the enhancement in the electrocatalytic performance of electrodes. Particularly, it can also achieve high binding force between the active material and the conductive substrate so as to prevent electroactive substance shedding. Thus, the composites can retain good stability and electrochemical performance when bended or twisted during the detection process, which is promising to be acted as flexible electrodes for wearable glucose sensors.

With the aim of developing the free-standing electrodes with higher electrocatalytic activity and flexibility, the $Cu_{50-x}Zr_{50}Ag_x$ (x = 0 and 7.5 at.%) metallic glasses (MGs) were designed as the dealloying precursor (note: the Cu-Zr-Ag MG containing 7.5 at% Ag is the optimized composition for fabricating the uniform bimetallic nanoporous substrate). Then, uniform nanowires grown on the nanoporous substrate were fabricated by dealloying and subsequently anodizing followed by heat treatment. It is observed that the morphology of copper-silver oxide nanowires (Cu_xO/Ag_2O, x = 1, 2) is different from copper monometallic oxide nanowires (Cu_xO). Furthermore, the Cu_xO/Ag_2O nanowire electrodes exhibit better glucose electrocatalytic performance and good flexibility as compared with Cu_xO. Ultimately, the possible mechanism of Cu_xO/Ag_2O electrode for glucose oxidation is also investigated.

2. Experimental

2.1. Synthesis of electrode modified by uniform nanowires

The typical synthesis process of in-situ grown nanowires on the nanoporous substrate is depicted in Fig. 1. Firstly, the $Cu_{50-x}Zr_{50}Ag_x$ (x = 0 and 7.5 at.%) alloy ingots were fabricated by melting the pure metal Cu (99.99%), Zr (99.99%) and Ag (99.99%) under the help of high-purity argon in the vacuum arc furnace. The metal glass precursor ribbons with a cross section of ~0.025 mm × 2 mm were prepared by a single-roller melt spinning. Subsequently, the as-spun $Cu_{50-x}Zr_{50}Ag_x$ (x = 0 and 7.5 at%) ribbons were dealloyed in 0.05 M HF solutions at about 298 K under the free corrosion. After dealloying the as-spun 0 at % Ag ribbon ($Cu_{50}Zr_{50}$) for 4 h and 7.5 at% Ag ribbon ($Cu_{42.5}Zr_{50}Ag_{7.5}$) for 8 h, nanoporous copper (NPC) and nanoporous copper silver (NP-CuAg) substrates were prepared, respectively. Then, the as-dealloyed samples were treated by anodizing in 0.5 M KOH with the current density of 15 mA/cm^2 for different oxidation time of 1 and 5 min. After that, the outcomes were rinsed three times with distilled water and further heated in muffle furnace at 200 °C for 2 h in the air. In this work, the self-standing Cu_xO or Cu_xO/Ag_2O (x = 1, 2) nanowire electrodes obtained by anodizing for 1 and 5 min, respectively, are represented as Cu_xO-1, Cu_xO-5, Cu_xO/Ag_2O-1 and Cu_xO/Ag_2O-5, respectively.

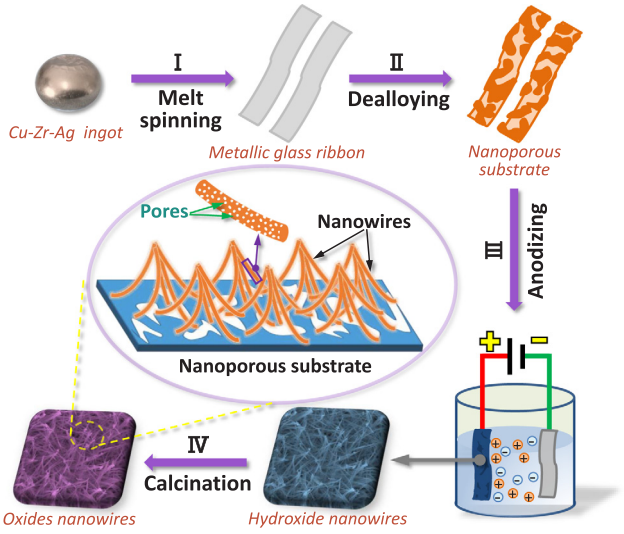

Fig. 1. Schematics of synthesis process of the free-standing and hierarchical porous electrode.

2.2. Microstructure characterization

The phases and crystal structures of the as-prepared samples were detected by X-ray diffractometer (XRD, Bruker D8, Cu-Kα) with the 2θ range of 25–85°. Transmission electron microscopy (TEM, Tecnai G2 F20) and scanning electron microscopy (SEM, Nova nanoSEM 450, FEI) equipped with an X-ray energy dispersive spectroscope (EDS) were applied to characterize the microstructure and morphology. X-ray photoelectron spectroscopy (XPS, Thermo Fisher Scientific) was used to investigate the surface chemical state and binding energy of Cu, Ag and O in the metallic oxide nanowires.

2.3. Electrochemical measurements

The electrochemical measurements were fulfilled on the electrochemical workstation (Chenhua CHI660E, China) with common three-electrode system at about 298 K. The anodized samples, commercial Pt net electrode and Ag/AgCl standard electrode (3 M KCl) were employed as the work electrode, the auxiliary electrode and the reference electrode, respectively. The cyclic voltammetry (CV) measurements were performed in the potential range from 0 to 0.8 V by the different scan rates and glucose concentrations. Note that current density is calculated based on geometric area. To evaluate the electrocatalytic performance of electrode, amperometric i-t curves were conducted by dripping glucose constantly into 0.2 M NaOH solution at the applied potential of 0.5 V. The frequency of electrochemical impedance spectroscopy (EIS) detections was conducted ranging from 0.01 to 10^6 Hz.

3. Results and discussion

3.1. Formation and structure of the composite electrodes

Fig. 2 displays the XRD patterns of the as-spun $Cu_{50-x}Zr_{50}Ag_x$ (x = 0 and 7.5 at%), corresponding as-dealloyed ribbons as well as the anodized samples after anodizing for 5 min followed by heat treatment. From Fig. 2a and b, it is found that both the as-spun 0 at% Ag ribbon ($Cu_{50}Zr_{50}$) and 7.5 at% Ag ribbon ($Cu_{42.5}Zr_{50}Ag_{7.5}$) have the broad diffraction halo peaks without sharp crystalline peak, showing the formation of amorphous structure. Moreover, no Zr element is detected in the as-dealloyed samples, implying that Zr element is selectively dissolved from $Cu_{50-x}Zr_{50}Ag_x$ (x = 0 and 7.5 at%) precursor ribbons, leaving the metal of Cu (x = 0 at%) and Cu-Ag (x = 7.5 at%) behind. After anodizing the as-dealloyed $Cu_{50}Zr_{50}$ for 5 min and further

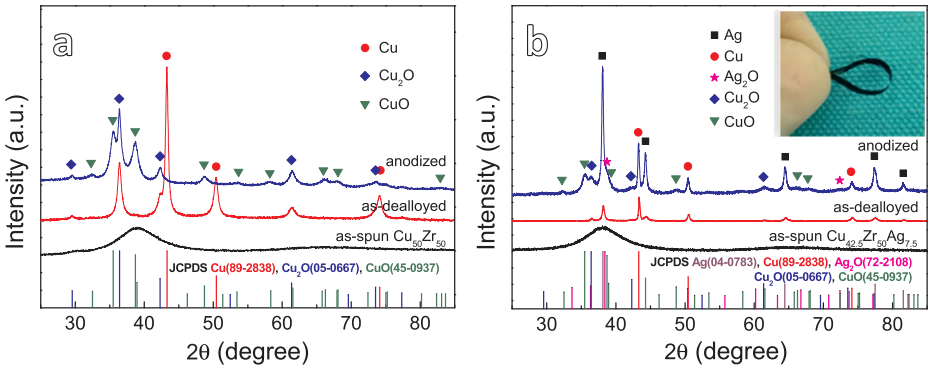

Fig. 2. (a) XRD patterns of the as-spun $Cu_{50}Zr_{50}$ ribbon, as-dealloyed sample immersed in 0.05 M HF for 4 h and anodized 5 min sample followed by heat treatment; (b) XRD patterns of the as-spun $Cu_{42.5}Zr_{50}Ag_{7.5}$ ribbon, as-dealloyed sample (NP-CuAg/MG) immersed in 0.05 M HF for 8 h and anodized 5 min sample followed by heat treatment with the photo of as-prepared sample.

calcination, the crystalline phases of anodized product in Fig. 2a is identified to be Cu_2O (JCPDS #05-0667) and CuO (JCPDS #45-0937), which demonstrates the formation of Cu_xO (x = 1, 2) on the NPC substrate. Similarly, for anodized 7.5 at% Ag sample (Fig. 2b), in addition to the diffraction peaks of metal Cu (JCPDS #89-2838) and Ag (JCPDS #04-0783) originating from the NP-CuAg substrate, the diffraction peaks for CuO (JCPDS #45-0937), Cu_2O (JCPDS #05-0667) and Ag_2O (JCPDS #72-2108) further confirm the formation of Cu_xO/Ag_2O (x = 1, 2) bimetallic oxides on the NP-CuAg substrate after anodization followed by heat treatment. Moreover, it is noticed that the anodized 0 at% Ag electrode is brittle and active material easily shed from the substrate under bending. On the contrary, the anodized 7.5 at % Ag electrode (the inset of Fig. 2b) illustrates well bendability without fracture at the great bending degree and the oxides layer is closely connected with the substrate, exhibiting good flexibility. This result indicates that the addition of Ag element to the dealloying precursor Cu-Zr MGs effectively improves the flexibility of the electrode material, which is promising as a wearable sensing materials in future.

XPS spectra (Fig. 3) are further measured to determine the oxidation valences of anodized samples for 5 min. From their typical wide-scan XPS spectra shown in Fig. 3a, it appears the presence of Cu and O elements in the anodized 0 at% Ag (Cu_xO-5) ribbon as well as the existence of Cu, Ag and O in the anodized 7.5 at% Ag (Cu_xO/Ag_2O-5) ribbon. The deconvolution of Cu 2p, Ag 3d, and O 1 s is presented in Fig. 3b–d. The two peaks of Cu $2p_{3/2}$ (Fig. 3b) are located at 932.7 eV and 934.0 eV together with the feature of two satellite peaks, which indicates the presence of Cu^+ and Cu^{2+} in both samples [32]. Ag 3d peaks of the anodized 7.5 at% Ag (Cu_xO/Ag_2O-5) ribbon is displayed in Fig. 3c. The two peaks located at 367.8 and 373.8 eV in conjunction with the binding energy interval of 6.0 eV are assigned to the characteristic Ag^+ $3d_{5/2}$ and Ag^+ $3d_{3/2}$ peaks, respectively, which is in agreement with the previous literature [33]. In Fig. 3d, the peaks of O 1 s are composed of three peaks and the corresponding binding energy is 529.3 eV, 530.6 eV and 531.3 eV. The lower binding energy at 529.3 eV is characteristic of OM corresponding to O^{2-} ions with transition metal oxides, while other peaks result from the OH groups and the water absorbed on the material surface [34]. As a result, the XPS results reveal that anodized sample surfaces on the nanoporous substrates are composed of Cu^+, Cu^{2+} oxides on NPC substrate and Cu^+, Cu^{2+} and Ag^+ oxides on NP-CuAg, which is consistent with XRD

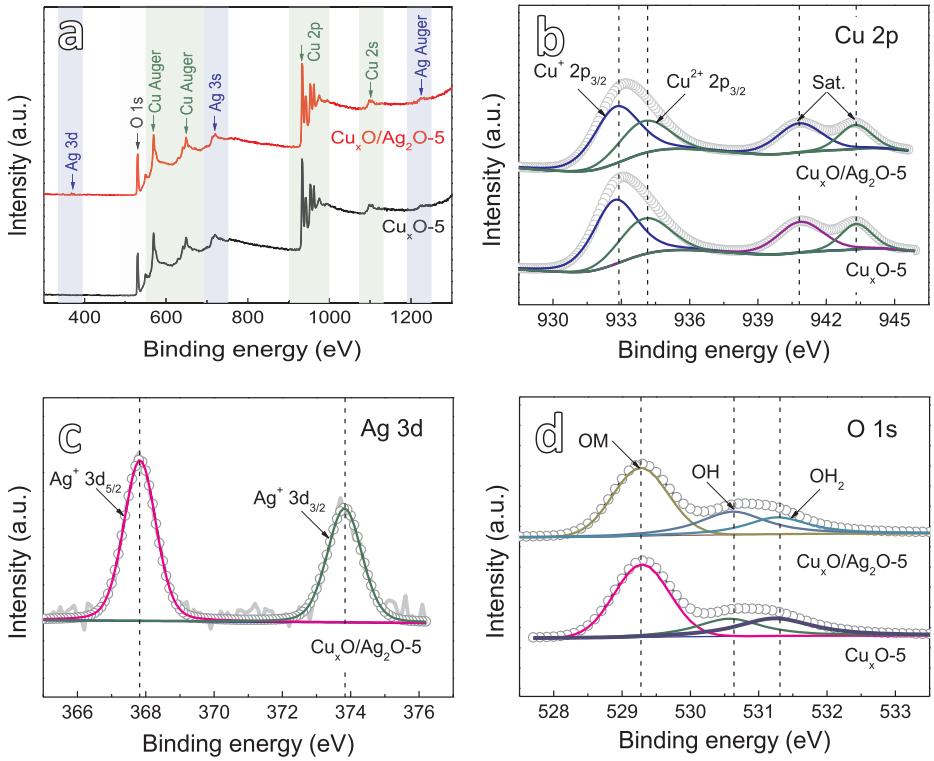

Fig. 3. (a) XPS spectra of anodized 5 min sample of Cu_xO and Cu_xO/Ag_2O; (b) Cu 2p of Cu_xO and Cu_xO/Ag_2O; (c) Ag 3d of Cu_xO/Ag_2O; (d) O 1 s of Cu_xO and Cu_xO/Ag_2O.

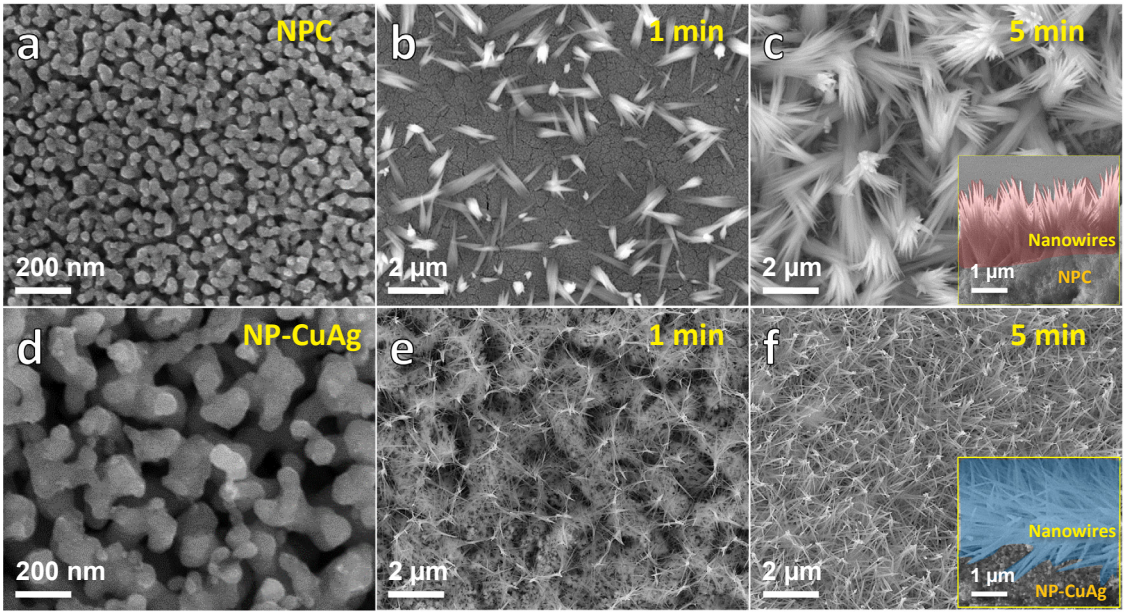

Fig. 4. Surface morphologies of (a) NPC; as-prepared Cu_xO sample anodized for (b) 1 min and (c) 5 min with the cross sectional morphology; Surface morphologies of (d) NP-CuAg; (b) the corresponding Cu_xO/Ag_2O composite after anodizing for (e) 1 min and 5 min with the inset of cross sectional morphology.

results.

Fig. 4 shows the surface morphologies of the as-prepared samples based on 0 at% Ag (Fig. 4a–c) and 7.5 at% Ag (Fig. 4d–f) precursors. In Fig. 4a and d, both the as-dealloyed ribbons (NPC and NP-CuAg) display an open, bicontinuous ligament-channel structure with different average ligament sizes of ~28 nm and ~100 nm, respectively. The well-ordered uniform nanoporous structure can act as substrate for anodizing and supply the source of metal for in-situ grown nanowires. In the Fig. 4b, the NPC anodized for 1 min (Cu_xO-1 electrode) presents sparse cluster-like structure assembled together by tens of ultrafine nanowires on the surface of NPC. When the anodization time increases up to 5 min, it is clearly found that a large number of Cu_xO nanowire clusters homogeneously grow on the NPC substrate (Fig. 4c). The nanowire clusters are much bigger and denser than those for 1 min. On the other hand, differing from the morphology of monometallic oxide nanowires (Cu_xO), it is very interesting to find that the bimetallic oxide nanowires (Cu_xO/Ag_2O-1 and Cu_xO/Ag_2O-5) (Fig. 4e and f) in-situ grown on the NP-CuAg substrate gather at the top of nanowires to form a star-like structure after anodizing. The formation of the top-converged structure is perhaps due to the bending of nanowires with large aspect ratios [35]. In the inset of Fig. 4c and f, nanowire layer with a thickness up to micrometers is seen to tightly combine with the nanoporous substrate. Remarkably, the Cu_xO/Ag_2O nanowires are more difficult to be scraped from the matrix than Cu_xO nanowires, which would benefit to improve the long-term stability of electrode. The EDS results for NP-CuAg and Cu_xO/Ag_2O-5 are further shown in Fig. S1. The nanoporous ligament of NP-CuAg shown in Fig. S1a consists of bimetallic copper and silver, which proves that the Zr element in the $Cu_{42.5}Zr_{50}Ag_{7.5}$ ribbon has been selectively dissolved during the dealloying process. Furthermore, it is found that the nanowires for Cu_xO/Ag_2O-5 (Fig. S1b) contains a large amount of O element in addition to the Cu and Ag, revealing that the oxides have formed after anodizing and calcining. The change of the chemical composition in the EDS agrees with XRD and XPS analysis.

It was reported that the dissolved metal ions integrate with OH^- in electrolyte during anodization, then aggregate on the defect of nanoporous metals [31,36,37]. Furthermore, the diffusion coefficient of Ag is one magnitude lower than that of Cu [38]. Therefore, it infers that the distinct discrepancy of two types of nanowire morphologies probably originates from different diffusion speed of Cu and Ag during anodizing. The lower diffusion rate of Ag ions may inhibit the spread of copper ions, resulting in the formation of different nanowire morphologies at the same oxidation time. Unfortunately, it is difficult to determine the complicated growth process and morphological evolution of two types of nanowires. Thus, more detailed analysis will be investigated in future.

TEM images provide more detailed compositions and structural characteristics of Cu_xO-5 (Fig. 5a–c) and Cu_xO/Ag_2O-5 (Fig. 5d–k) nanowires at high-magnification. It can be observed in Fig. 5a and d that the diameters of Cu_xO-5 and Cu_xO/Ag_2O-5 nanowires are about 10–30 nm and 15–60 nm, respectively. Moreover, there are many smaller nanopores on the each nanowire with the sizes of 1–3 nm (Fig. 5b and e). which generally causes from the gas release during the calcination process. Additionally, it is not seen the nanopores in the TEM image (Fig. S2) of the Cu_xO/Ag_2O-5 nanowire obtained before calcination, which further proves that the nanopore formation on the nanowires is caused by calcination. As illustrated in Fig. 5c, the lattice spacings of 0.246 and 0.253 nm are ascribed to the (1 1 1) planes of Cu_2O and (0 0 2) planes of CuO, respectively. Lattice spacings measured in Fig. 5f are 0.246, 0.253 and 0.234 nm corresponding to the (1 1 1) plane of Cu_2O, (0 0 2) plane of CuO and (0 1 1) plane of Ag_2O. Furthermore, the selected-area electron diffraction (SAED) patterns for nanowires (the set of Fig. 5c and f) own good polycrystallinity character and agree with the spacing of the lattice spacing. The TEM image of Cu_xO/Ag_2O-5 nanowire (Fig. 5g) was selected to further analyze the distribution of elements. It is found from Fig. 5h–k that O, Cu and minor Ag atoms are uniformly distributed on Cu_xO/Ag_2O nanowire. These results of TEM and SEM further demonstrate that as-prepared nanowires anodized on the nanoporous substrate are composed of Cu or Ag oxides and have a hierarchical porous structure, i.e., the nanopores of the substrate, small pores on the each nanowire and the micropores arising from the nanowires interlacing.

The pore-size distribution of the Cu_xO-5 and Cu_xO/Ag_2O-5 displayed in the inset of the Fig. 6 mainly ranges from 1 to 10 nm. Moreover, the peak intensity of Cu_xO/Ag_2O-5 is higher than that of Cu_xO-5. According to their N_2 absorption-desorption isotherms (Fig. 6), the BET specific surface area of the Cu_xO/Ag_2O-5 (~31.22 $m^2\ g^{-1}$) is larger than that of the Cu_xO-5 electrode (20.02 $m^2\ g^{-1}$). The high porosity and large specific surface area of Cu_xO/Ag_2O-5 would be beneficial to provide more electrocatalytic active sites for glucose

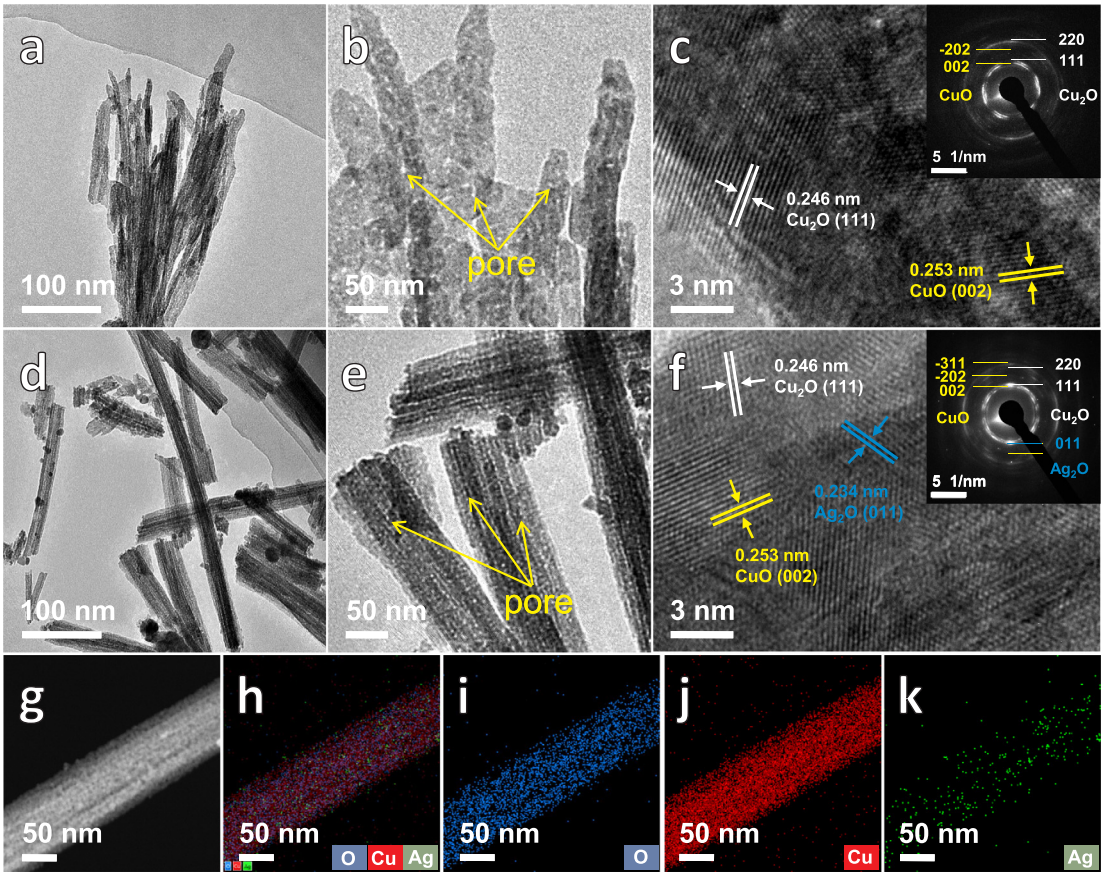

Fig. 5. TEM images of (a, b) Cu_xO-5 nanowires; (c) the corresponding HRTEM image with SAED pattern; TEM images of (d, e) Cu_xO/Ag_2O-5 nanowires; (f) the corresponding HRTEM image with SAED pattern; (g) the selected region of Cu_xO/Ag_2O-5 nanowire for EDS; EDS elemental mapping images of (h) mix of O, Cu and Ag; (i) O; (j) Cu; (k) Ag.

detection.

3.2. Electrocatalytic performance of the electrode composites

Cyclic voltammetry tests were performed to analyze the glucose sensing performance of as-prepared 0 at% Ag electrode. Fig. 7a represents the CVs of the NPC, Cu_xO-1 and Cu_xO-5 in 0.2 M NaOH solution with or without 1 mM glucose at a scan rate of 50 mV/s. It can be seen that the anodic oxidation current signals of all electrodes increase when glucose was added in NaOH solution as compared to those without glucose, indicating Cu_xO electrodes show glucose sensing performance. Moreover, the current signal response of Cu_xO-5 is clearly higher than those of NPC and Cu_xO-1. These results reveal that the existence of nanowires effectively enhances the electrochemical performance of material. Meanwhile, the electrocatalytic activity of electrode towards glucose is improved with increasing anodization time. Fig. 7b shows the CV curves of the Cu_xO-5 electrode with different concentrations of glucose (from 1 to 10 mM). It appears that there is a distinct anodic oxidation peak located at around 0.5 V. Furthermore, the oxidation current response rises with an increase in the glucose concentration. The result indicates that CuxO-5 electrode does have the good glucose sensing performance. Fig. 7c shows CV curves of the Cu_xO-5 composite material in 0.2 M NaOH with 1 mM glucose at different scan rates. The reaction current increases as the scan rates rise from 10 to 100 mV/s. The relationship of the oxidation current obtained around 0.5 V and the square root of scan rate satisfies positive linear correlation (R^2 = 0.996), revealing that the glucose oxidation is a diffusion control process, which is good for quantitative analysis in real detections [39]. In addition, the tests for as-prepared 7.5 at% Ag nanowire electrode (Cu_xO/Ag_2O-5) show the similar electrochemical

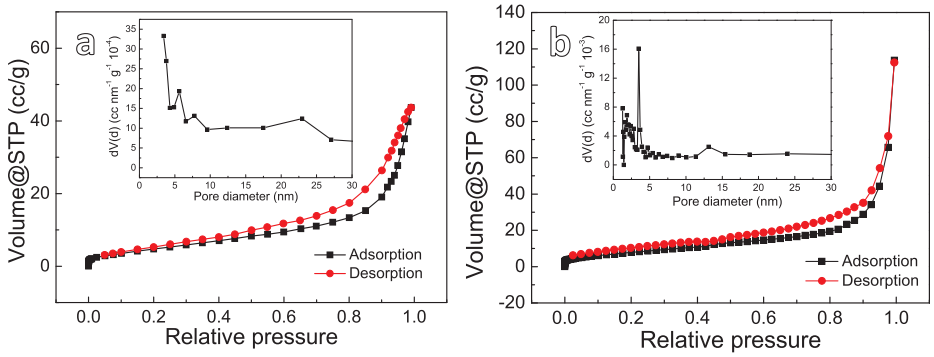

Fig. 6. N_2 adsorption-desorption isotherms with the pore-size distribution of (a) Cu_xO-5; (b) Cu_xO/Ag_2O-5.

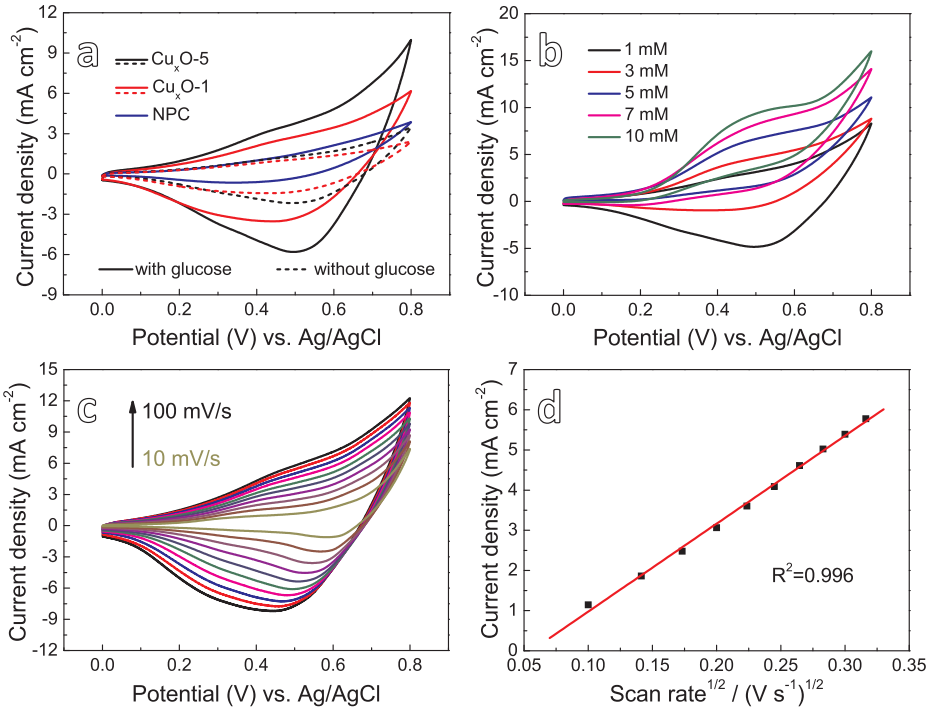

Fig. 7. (a) The CVs of NPC, Cu_xO-1 and Cu_xO-5 electrodes in 0.2 M NaOH with or without 1 mM glucose; (b) CV with different concentrations of glucose of Cu_xO-5 electrode; (c) CV at scan rates of 10, 20, 30, 40, 50, 60, 70, 80, 90, 100 mV s^{-1} for Cu_xO-5 electrode in 0.2 M NaOH with 1 mM glucose; (d) the calibration curve of anodic current density obtained around 0.5 V and square root of scan rate.

behaviors (Fig. S3), which further demonstrates that the in-situ growth of nanowires on the nanoporous substrate is effective in improving the oxidation performance of glucose.

Amperometric i-t curves were conducted to further investigate the sensitivity of as-fabricated composite electrodes. Fig. 8a shows the changes in the current density as a function of time with dropping 1 mM glucose solutions in the 0.2 M NaOH every 50 s. It appears that both the Cu_xO and Cu_xO/Ag_2O electrode have significant current response signals when 1 mM glucose is added. Subsequently, the corresponding linear fitting of current density and concentration (Fig. 8b) for all electroactive materials exhibits a wide line range up to 15 mM. Particularly, the Cu_xO/Ag_2O-5 has the highest sensitivity reaching to 1.31 mA $mM^{-1}cm^{-2}$ and the low detection limit of 0.5 μM calculated by LOD = $3\sigma_b/m$, where σ_b is the standard deviation of the blank sample and m is the slope of the calibration graph [40]. It reveals that the synergistic effect of Cu and Ag element is conducive to improve the glucose electrocatalytic properties of materials. Fig. 8c shows the Nyquist plots of Cu_xO-5 and Cu_xO/Ag_2O-5 in 0.2 M NaOH with 1 mM glucose. The measured radius of the semicircle for the Cu_xO/Ag_2O-5 electrode is much smaller than that for Cu_xO-5, indicating that Cu_xO/Ag_2O-5 has a faster charge transfer rate than Cu_xO-5 during the glucose oxidation process [41]. The EIS result confirms that addition of Ag element effectively enhances the conductivity of the electrode composites, resulting in excellent electrocatalytic performance. Besides, the

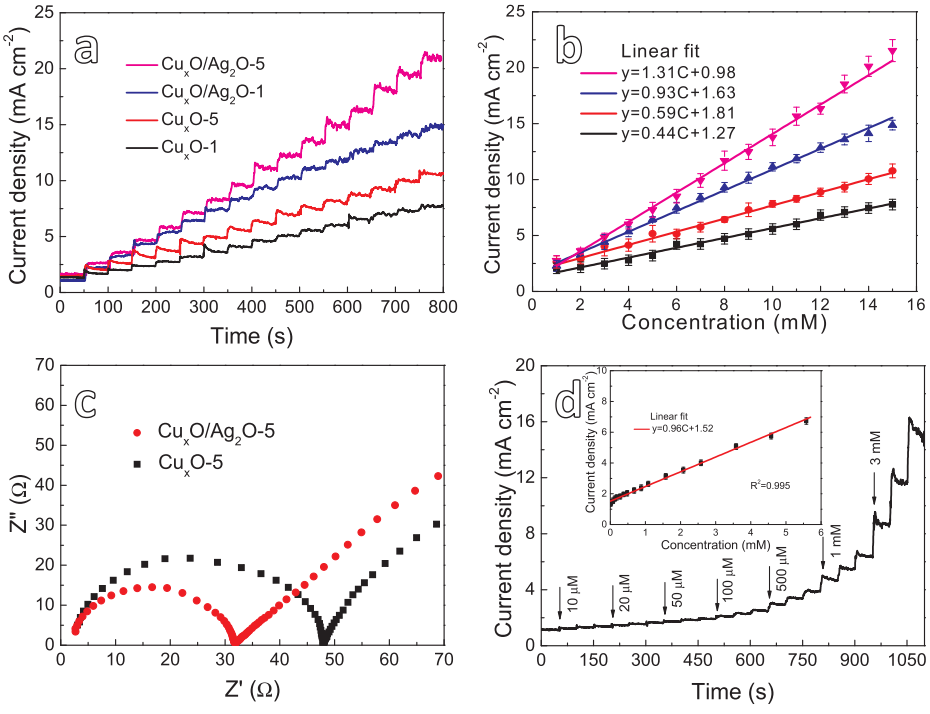

Fig. 8. (a) Amperometric response curve (i-t curve) with successive additions of 1 mM glucose into 0.2 M NaOH solution at 0.5 V; (b) the corresponding glucose calibration curves for (a); (c) EIS of the Cu_xO-5 and Cu_xO/Ag_2O-5 electrode measured in 0.2 M NaOH with 1 mM glucose; (d) the i-t curve of Cu_xO/Ag_2O-5 at low glucose concentration with the inset showing corresponding calibration curve.

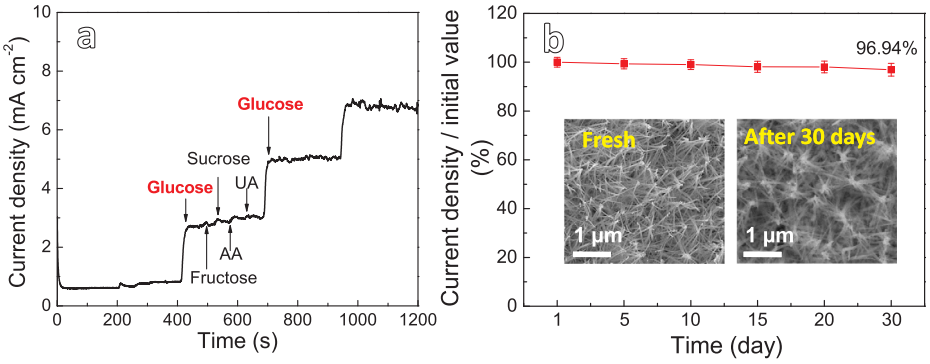

Fig. 9. (a) Anti-interference ability study of Cu_xO/Ag_2O-5 electrode, amperometric i-t curve of the Cu_xO/Ag_2O-5 electrode with successive addition of 0.1 mM interfering species (fructose, sucrose, ascorbic acid (AA), uric acid (UA)), and 3 mM glucose into 0.2 M NaOH at an applied potential of 0.5 V; (b) the change of current response of the Cu_xO/Ag_2O-5 electrode after 30 day-repeated experiments with the inset of the surface morphology before and after experiment.

current response signal of Cu_xO/Ag_2O-5 (Fig. 8d) at low glucose concentration was detected by dropping various concentration of glucose from 10 μM to 5 mM. The corresponding fit curve was obtained in the inset of Fig. 8d. It is calculated that the sensitivity is about 0.95 mA mM^{-1} cm^{-2} (from 0.02 to 5.58 mM). This result reveals that the NP-CuAg substrate surface modified by Cu_xO/Ag_2O-5 nanowires is very suitable to the electrochemical detection of lower concentration glucose.

It should be noted that glucose often coexists with small amount of organic molecules (such as ascorbic acid (AA), uric acid (UA), fructose and sucrose) in human blood. These organic substances also generate corresponding current signals during practical application, which would interfere glucose detecting result. Thus, it is necessary for electrode material to have good anti-interference ability. In order to study the anti-interference ability of the Cu_xO/Ag_2O-5 electrode, 0.1 mM AA, 0.1 mM UA, 0.1 mM fructose, 0.1 mM sucrose, and 3 mM glucose were successively added into stirred 0.2 M NaOH solution [42,43]. As shown in Fig. 9a, the addition of glucose brings about a significant current response for Cu_xO/Ag_2O-5, while the current signals of the interferences (fructose, sucrose, AA and UA) are neglectable, illustrating the excellent anti-interference ability of Cu_xO/Ag_2O-5 against above-mentioned small amount of interfering species. The relative standard deviation (RSD) of the sensitivity for 1 mM glucose which measured with the same electrode for 3 times is ~2.36%, which indicates that the Cu_xO/Ag_2O-5 electrode possesses good intra-electrode repeatability. Moreover, the current response detected for six Cu_xO/Ag_2O-5 electrodes with the same preparation process are similar (Fig. S4), revealing the outstanding inter-electrode reproducibility. In addition, the long-term stability of the Cu_xO/Ag_2O-5 was also examined in this work. The composite was exposed in air, and the current response to 1 mM glucose was detected once a day during the period of 30 days. Fig. 9b shows the results normalized with the initial value. It is found that the current response of electrode on the 30th day still remains about 96.94% with the sensitivity of 1.25 mA mM^{-1} cm^{-2}, which confirms that it has superior long-term stability to satisfy long-term practical applications. Subsequently, the surface morphology of Cu_xO/Ag_2O-5 before and after 30 days was further characterized by SEM. As shown in the inset of Fig. 9b, the Cu_xO/Ag_2O-5 nanowires after storage for 30 days still retain the top-converged structure and good integrity, implying well combination force between Cu_xO/Ag_2O-5 nanowires and substrate. However, Cu_xO-5 nanowires are easy to fall off as compared to Cu_xO/Ag_2O-5. The result demonstrates that addition of Ag is beneficial to enhance the combination force between the nanowires and the substrate, thus avoiding active substance flaking away.

Table 1 lists comparison of glucose electrocatalytic performance among different materials [44–49]. It is seen that the Cu_xO/Ag_2O-5 composite developed in this work has excellent electrocatalytic activity such as wide linear range, high sensitivity and low detection limit. Compared with powdery composites and Ag/CuO NFs/indium tin oxide (ITO) [44–46,48,49], the preparation process of the Cu_xO/Ag_2O-5 composites is simple and cost-effective. Most importantly, in-situ growth method for preparing the binder-free and self-standing Cu_xO/Ag_2O-5 electrode could effectively strengthen the interface bonding force between the NP-CuAg and nanowires, and prevent active materials from flaking off. Moreover, the hierarchical porous structure of the Cu_xO/Ag_2O-5 electrode not only offers more reactive sites, but also promotes the transportation of electrons and ions, thereby enhancing electrocatalytic performance. It is particularly worth noting that the Cu_xO/Ag_2O-5 electrode behaves good flexibility, which has been rarely reported so far. Although the CuO NWA grown on Cu foil listed in Table 1 [47] is also a free-standing electrode with good flexibility, the present Cu_xO/Ag_2O-5 electrode shows wider linear range, which is good for the practical application in glucose detection. Accordingly, the present Cu_xO/Ag_2O-5 electrode with hierarchical porous structure, superb electrocatalytic property and good flexibility is expected to facilitate the development of wearable glucose sensors.

To make clear the reasons why the present Cu_xO/Ag_2O-5 composite electrode demonstrates the outstanding electrocatalytic performance, the possible electrocatalytic mechanism of free-standing Cu_xO/Ag_2O-5 electrode is shown in the Fig. 10. It is well known that the structure and ingredient of electrode material significantly affect the electrocatalytic properties for glucose. In term of structure, the Cu_xO/Ag_2O-5 nanowire electrode possesses the hierarchical porous architecture, consisting of the micropores on Cu_xO/Ag_2O nanowires, the rich macropore space arising from interlaced nanowires as well as the nanopores of the NP-CuAg substrate, which provide more active sites and achieve effective contact of the electrode/electrolyte interfaces. Besides, for the present Cu_xO/Ag_2O-5 electrode during reaction, the Cu(I/II) or Ag(I) of Cu_xO/Ag_2O nanowires are oxidized to Cu(III) or Ag(II) served as an important intermediate of glucose conversion gluconic acid. Meanwhile, electrons produced by oxidizing are shifted from nanowires to NP-CuAg substrate, generating relevant current response signal. Subsequently, the Cu(III) or Ag(II) is reduced to Cu(I/II) or Ag(I) for recycling during reactions [50–52]. Therefore, the redox couples of Cu and Ag play an important role in glucose electrooxidation process. In addition, the nanowires consisting simultaneously of Cu_xO and Ag_2O could realize the synergistic effect of Cu and Ag element, which remarkably enhances the glucose electrocatalytic activity by the mutual promotion and endues the electrode with superior conductivity for efficient electron transportation. In summary, the newly developed Cu_xO/Ag_2O-5 composite electrode with good flexibility and outstanding electrocatalytic performance is a promising glucose sensing material in the field of wearable.

4. Conclusions

In this work, we have successfully prepared the free-standing Cu_xO and Cu_xO/Ag_2O (x = 1, 2) composite electrodes by dealloying $Cu_{50-x}Zr_{50}Ag_x$ (x = 0 and 7.5 at%), along with anodizing and heat treatment. Two types of electrodes with the morphology of nanowires present a hierarchical porous structure. Different from the cluster-like Cu_xO nanowires anodized on NPC, the Cu_xO/Ag_2O nanowires anodized on NP-

Table 1
Comparison of glucose electrocatalytic performance among different materials.

Materials	Sample state	Flexibility	Linear range	Sensitivity (μA mM^{-1} cm^{-2})	Detection limit (μM)	Stability	Ref.
CuO/Cu_2O-NF	Powders/GCE	—	0.5–10 mM	830	0.7	—	[44]
CuO@CuNWs	Template/GCE	—	1–10 mM	1250.8	0.69	94% (20 days)	[45]
Porous CuO	Powders/GCE	—	0.5–2.8 mM	934.2	0.1	96.6% (7 days)	[46]
CuO NWA	Cu foil (in-situ growth)	Good	up to 2.55 mM	1420.3	5.1	98% (30 days)	[47]
Ag NPs	Powders/GCE	—	1–8.9 mM	895.8	0.0048	96% (10 days)	[48]
Ag/CuO NFs	ITO (ex-situ growth)	—	0.5–0.5 mM	1347	0.05	93% (30 days)	[49]
Cu_xO/Ag_2O-5	Ribbon (in-situ growth)	Good	up to 15 mM	1310	0.5	96.94% (30 days)	This work

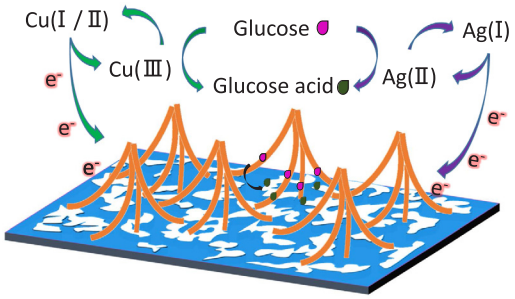

Fig. 10. Schematic illustration of glucose electrocatalytic mechanism by Cu_xO/Ag_2O-5 electrode.

CuAg substrate have the feature of top-converged. In addition, benefiting from the addition of Ag element, the Cu_xO/Ag_2O-5 composites display good flexibility and well electrocatalytic performance for glucose. The high sensitivity is about 1.31 mA mM^{-1} cm^{-2} with the low detection limit of 0.5 μM. The wide linear range up to 15 mM together with good anti-interference ability and stability. The excellent glucose sensing performance is primarily ascribed to the hierarchical porous structure and the synergistic effect of Cu and Ag elements. Accordingly, the Cu_xO/Ag_2O-5 composite electrode with highly improved electrocatalytic performance and good flexibility is promising to apply in the development of wearable glucose sensors.

CRediT authorship contribution statement

Qian Zhang: Methodology, Investigation, Validation, Formal analysis, Writing - original draft. **Man Li:** Methodology, Investigation, Validation, Data curation, Formal analysis. **Zhifeng Wang:** Writing - review & editing, Supervision, Resources. **Chunling Qin:** Conceptualization, Writing - review & editing, Supervision, Funding acquisition. **Mengmeng Zhang:** Validation, Data curation. **Yongyan Li:** Writing - review & editing, Supervision.

Declaration of Competing Interest

The authors declare that they have no known competing financial interests or personal relationships that could have appeared to influence the work reported in this paper.

Acknowledgments

This work is financially supported by the National Natural Science Foundation of China (51671077) and Key Project of Science & Technology Research of Higher Education Institutions of Hebei Province, China (ZD2018059).

Appendix A. Supplementary material

Supplementary data to this article can be found online at https://doi.org/10.1016/j.apsusc.2020.146062.

References

[1] L.Y. Lin, B.B. Karakocak, S. Kavadiya, T. Soundappan, P. Biswas, A highly sensitive non-enzymatic glucose sensor based on $Cu/Cu_2O/CuO$ ternary composite hollow spheres prepared in a furnace aerosol reactor, Sensor. Actuator. B Chem. 259 (2018) 745–752.
[2] W.W. Li, R.Z. Ouyang, W.Y. Zhang, S. Zhou, Y. Yang, Y.J. Ji, Y. Yang, K. Feng, X.C. Liang, M.S. Xiao, Y.Q. Miao, Single walled carbon nanotube sandwiched Ni-Ag hybrid nanoparticle layers for the extraordinary electrocatalysis toward glucose oxidation, Electrochim. Acta 188 (2016) 197–209.
[3] S.L. Liu, W. Zeng, Y.Q. Li, Synthesis of $ZnCo_2O_4$ microrods grown on nickel foam for nonenzymatic glucose sensing, Mater. Lett. 259 (2020) 126820.
[4] L. Zhang, H. Li, Y.H. Ni, J. Li, K.M. Liao, G.C. Zhao, Porous cuprous oxide microcubes for non-enzymatic amperometric hydrogen peroxide and glucose sensing, Electrochem. Commun. 11 (2009) 812–815.
[5] H.X. Yang, Z.H. Wang, C.C. Li, C.X. Xu, Nanoporous PdCu alloy as an excellent electrochemical sensor for H_2O_2 and glucose detection, J. Colloid Interf. Sci. 491 (2017) 321–328.
[6] X. Wang, M.Z. Wang, S.Y. Feng, D.P. He, P. Jiang, Controlled synthesis of flower-like cobalt phosphate microsheet arrays supported on Ni foam as a highly efficient 3D integrated anode for non-enzymatic glucose sensing, Inorg. Chem. Front. 7 (2020) 108–116.
[7] Y.C. Zhang, L. Su, D. Manuzzi, H.V.E. de los Monteros, W.Z. Jia, D.Q. Huo, C.J. Hou, Y. Lei, Ultrasensitive and selective non-enzymatic glucose detection using copper nanowires, Biosens. Bioelectron. 31 (2012) 426–432.
[8] I. Potzelberger, A.I. Mardare, A.W. Hassel, Non-enzymatic glucose sensing on copper-nickel thin film alloy, Appl. Surf. Sci. 417 (2017) 48–53.
[9] Y. Li, M.W. Xie, X.P. Zhang, Q. Liu, D.M. Lin, C.G. Xu, F.Y. Xie, X.P. Sun, Co-MOF nanosheet array: a high-performance electrochemical sensor for non-enzymatic glucose detection, Sens. Actuator. B Chem. 278 (2019) 126–132.
[10] S.Y. Dong, Q.X. Yang, L. Peng, Y. Fang, T.L. Huang, Dendritic Ag@Cu bimetallic interface for enhanced electrochemical responses on glucose and hydrogen peroxide, Sens. Actuator. B Chem. 232 (2016) 375–382.
[11] X.J. Liu, L. Long, W.X. Yang, L.L. Chen, J.B. Jia, Facilely electrodeposited coral-like copper micro-/nano-structure arrays with excellent performance in glucose sensing, Sens. Actuator. B Chem. 266 (2018) 853–860.
[12] G.L. Zhang, K.S. Ming, J.L. Kang, Q. Huang, Z.J. Zhang, X.R. Zheng, X.F. Bi, High entropy alloy as a highly active and stable electrocatalyst for hydrogen evolution reaction, Electrochim. Acta 279 (2018) 19–23.
[13] Y.Y. Zhou, M.Y. Niu, S.L. Zhu, Y.Q. Liang, Z.D. Cui, X.J. Yang, A. Inoue, Preparation and electrocatalytic performance of nanoporous Pd/Sn and Pd/Sn-CuO composite catalysts, Electrochim. Acta 296 (2019) 397–406.
[14] Z.N. Liu, L.H. Huang, L.L. Zhang, H.Y. Ma, Y. Ding, Electrocatalytic oxidation of d-glucose at nanoporous Au and Au-Ag alloy electrodes in alkaline aqueous solutions, Electrochim. Acta 54 (2009) 7286–7293.
[15] T.J. Meng, H.X. Jia, H.M. Ye, T. Zeng, X.J. Yang, H. Wang, Y.F. Zhang, Facile preparation of $CoMoO_4$ nanorods at macroporous carbon hybrid electrocatalyst for non-enzymatic glucose detection, J. Colloid Interf. Sci. 560 (2020) 1–10.
[16] Y.C. Zhang, Y.X. Liu, L. Su, Z.H. Zhang, D.Q. Huo, C.J. Hou, Y. Lei, CuO nanowires based sensitive and selective non-enzymatic glucose detection, Sens. Actuator. B Chem. 191 (2014) 86–93.
[17] X.W. Wu, F. Chen, M. Huang, Z.H. Dan, F.X. Qin, Ni-decorated ZrAlCo-O nanotube arrays with ultrahigh sensitivity for non-enzymatic glucose sensing, Electrochim. Acta 311 (2019) 201–210.
[18] D.L. Zhou, J.J. Feng, L.Y. Cai, Q.X. Fang, J.R. Chen, A.J. Wang, Facile synthesis of monodisperse porous Cu_2O nanospheres on reduced graphene oxide for non-enzymatic amperometric glucose sensing, Electrochim. Acta 115 (2014) 103–108.
[19] H.P. Yang, G.W. Gao, F. Teng, W.J. Liu, S.J. Chen, Z.C. Ge, Nickel hydroxide nanoflowers for a nonenzymatic electrochemical glucose sensor, J. Electrochem. Soc. 161 (2014) 216–219.
[20] M. Li, Z.F. Wang, Q. Zhang, C.L. Qin, A. Inoue, W.B. Guo, Formation and evolution of ultrathin Cu_2O nanowires on NPC ribbon by anodizing for photocatalytic degradation, Appl. Surf. Sci. 506 (2020) 144819.
[21] Y. Ding, Y. Wang, L. Su, H. Zhang, Y. Lei, Preparation and characterization of NiO-Ag nanofibers, NiO nanofibers, and porous Ag: towards the development of a highly sensitive and selective non-enzymatic glucose sensor, J. Mater. Chem. 20 (2010) 9918–9926.
[22] L.C. Jiang, W.D. Zhang, A highly sensitive nonenzymatic glucose sensor based on CuO nanoparticles-modified carbon nanotube electrode, Biosens. Bioelectron. 25 (2010) 1402–1407.

[23] M.M. Liu, R. Liu, W. Chen, Graphene wrapped Cu_2O nanocubes: Non-enzymatic electrochemical sensors for the detection of glucose and hydrogen peroxide with enhanced stability, Biosens. Bioelectron. 45 (2013) 206–212.
[24] J. Lv, C.C. Kong, Y. Xu, Z.M. Yang, X.J. Zhang, S.C. Yang, G. Meng, J.H. Li, S. Yang, Facile synthesis of novel CuO/Cu_2O nanosheets on copper foil for high sensitive nonenzymatic glucose biosensor, Sens. Actuator. B Chem. 248 (2017) 630–638.
[25] J.H. Li, J.B. Jiang, Z.F. Xu, M.Q. Liu, S.P. Tang, C.M. Yang, D. Qian, Facile synthesis of Ag@Cu_2O heterogeneous nanocrystals decorated N-doped reduced graphene oxide with enhanced electrocatalytic activity for ultrasensitive detection of H_2O_2, Sens. Actuator. B Chem. 260 (2018) 529–540.
[26] C.H. Wei, C.X. Kang, Q.M. Liu, Ag nanosheets grown on Cu nanowire-based flexible films for sensitive non-enzymatic glucose sensors, Nanotechnology 31 (2020) 115501.
[27] H. Li, C.Y. Guo, C.L. Xu, A highly sensitive non-enzymatic glucose sensor based on bimetallic Cu-Ag superstructures, Biosens. Bioelectron. 63 (2015) 339–346.
[28] B. Fang, A.X. Gu, G.F. Wang, W. Wang, Y.H. Feng, C.H. Zhang, X.J. Zhang, Silver oxide nanowalls grown on Cu substrate as an enzymeless glucose sensor, ACS Appl. Mater. Inter. 1 (2009) 2829–2834.
[29] F.D. Franco, A. Zaffora, M. Santamaria, F.D. Quarto, Anodization and anodic oxides, Encyclopedia of Interfacial, Chemistry (2018) 26–40.
[30] C.Q. Dong, X.J. Yan, C.H. Si, H. Gao, W.S. Ma, G.H. Cheng, W.F. Yang, H. Zhang, Z.H. Zhang, New-type nickel oxalate nanostructures for ultrahigh sensitive electrochemical biosensing of glucose, Adv. Mater. Interfaces (2016) 1600197.
[31] M. Li, Y.Y. Li, Q. Zhang, C.L. Qin, W.M. Zhao, Z.F. Wang, A. Inoue, Ultrafine Cu_2O/CuO nanosheet arrays integrated with NPC/BMG composite rod for photocatalytic degradation, Appl. Surf. Sci. 483 (2019) 285–293.
[32] N.S. Mclntyre, M.G. Cook, X-Ray photoelectron studies on some oxides and hydroxides of cobalt, nickel, and copper, Anal. Chem. 47 (1975) 2208–2213.
[33] C.L. Yu, G. Li, S. Kumar, K. Yang, R.C. Jin, Phase transformation synthesis of novel Ag_2O/Ag_2CO_3 heterostructures with high visible light efficiency in photocatalytic degradation of pollutants, Adv. Mater. 26 (2014) 892–898.
[34] C.L. Qin, D.H. Zheng, Q.F. Hu, X.M. Zhang, Z.F. Wang, Y.Y. Li, J.S. Zhu, J.Z. Ou, C.H. Yang, Y.C. Wang, Flexible integrated metallic glass-based sandwich electrodes for high-performance wearable all-solid-state supercapacitors, Appl. Mater. Today 19 (2020) 100539.
[35] F. Maurer, A. Dangwal, D. Lysenkov, G. Muller, M.E. Toimil-Molares, C. Trautmann, J. Brotz, H. Fuess, Field emission of copper nanowires grown in polymer ion-track membranes, Nucl. Instrum. Meth. B 245 (2006) 337–341.
[36] D.H. Zheng, F. Zhao, Y.Y. Li, C.L. Qin, J.S. Zhu, Q.F. Hu, Z.F. Wang, A. Inoue, Flexible NiO micro-rods/nanoporous Ni/metallic glass electrode with sandwich structure for high performance supercapacitors, Electrochim. Acta 297 (2019) 767–777.
[37] Z.F. Wang, Y.S. Zhang, H.Q. Xiong, C.L. Qin, W.M. Zhao, X.Z. Liu, Yucca fern shaped CuO nanowires on Cu foam for remitting capacity fading of Li-ion battery anodes, Sci. Rep. 8 (2018) 6530.
[38] J. Erlebacher, An atomistic description of dealloying porosity evolution, the critical potential, and rate-limiting behavior, J. Electrochem. Soc. 151 (2004) C614–C626.
[39] Z.J. Zhuang, X.D. Su, H.Y. Yuan, Q. Sun, D. Xiao, M.M.F. Choi, An improved sensitivity non-enzymatic glucose sensor based on a CuO nanowire modified Cu electrode, Analyst 133 (2008) 126–132.
[40] R. Li, X.J. Liu, H. Wang, Y. Wu, Z.P. Lu, High-performance hybrid electrode decorated by well-aligned nanograss arrays for glucose sensing, Biosens. Bioelectron. 102 (2018) 288–295.
[41] X. Ke, Y.T. Xu, C.C. Yu, J. Zhao, G.F. Cui, D. Higgins, Z.W. Chen, Q. Li, H. Xu, G. Wu, Pd-decorated three-dimensional nanoporous Au/Ni foam composite electrodes for H_2O_2 reduction, J. Mater. Chem. A 2 (2014) 16474.
[42] A. Ahmadalinezhad, S. Chatterjee, A.C. Chen, Synthesis and electrochemical study of nanoporous palladium-cadmium networks for non-enzymatic glucose detection, Electrochim. Acta 112 (2013) 927–932.
[43] J. Luo, S.S. Jiang, H.Y. Zhang, J.Q. Jiang, X.Y. Liu, A novel non-enzymatic glucose sensor based on Cu nanoparticle modified graphene sheets electrode, Anal. Chim. Acta 709 (2012) 47–53.
[44] N. Lu, C.L. Shao, X.H. Li, T. Shen, M.Y. Zhang, F.J. Miao, P. Zhang, X. Zhang, K.X. Wang, Y. Zhang, Y.C. Liu, CuO/Cu_2O nanofibers as electrode materials for non-enzymatic glucose sensors with improved sensitivity, RSC Adv. 4 (2014) 31056.
[45] J.P. Dong, L.X. Ren, Y. Zhang, X.L. Cui, P.F. Hu, J.Q. Xu, Direct electrodeposition of cable-like CuO@Cu nanowires array for non-enzymatic sensing, Talanta 132 (2015) 719–726.
[46] L.L. Li, Y.Y. Liu, L.H. Ai, J. Jiang, Synthesis of the crystalline porous copper oxide architectures derived from metal-organic framework for electrocatalytic oxidation and sensitive detection of glucose, J. Ind. Eng. Chem. 70 (2019) 330–337.
[47] J.F. Huang, Y.H. Zhu, X.L. Yang, W. Chen, Y. Zhou, C.Z. Li, Flexible 3D porous CuO nanowire arrays for enzymeless glucose sensing: in situ engineered versus ex situ piled, Nanoscale 7 (2015) 559–569.
[48] T. Dayakar, K.V. Rao, J. Park, K.K. Sadasivuni, K.R. Rao, N.J. Rambabu, Non-enzymatic biosensing of glucose based on silver nanoparticles synthesized from ocimum tenuiflorum leaf extract and silver nitrate, Mater. Chem. Phys. 216 (2018) 502–507.
[49] Y. Xie, Y.H. Song, Y.Y. Zhang, L.J. Xu, L.F. Miao, C.W. Peng, L. Wang, A sensitive AgNPs/CuO nanofibers non-enzymatic glucose sensor based on electrospinning technology, Sens. Actuator. B Chem. 195 (2014) 431–438.
[50] J. Wang, W.D. Zhang, Fabrication of CuO nanoplatelets for highly sensitive enzyme-free determination of glucose, Electrochim. Acta 56 (2011) 7510–7516.
[51] H.M. Quan, S.U. Park, J.M. Park, Electrochemical oxidation of glucose on silver nanoparticle-modified composite electrodes, Electrochim. Acta 55 (2010) 2232–2237.
[52] D.M. Zhu, C.Q. Xia, Z.D. Yang, X.H. Wang, T. Yang, C.Y. Liang, F.X. Yin, Q. Li, Fabrication of non-enzyme glucose sensor via dealloying amorphous Zr-Cu alloy and anodic oxidation, Mater. Lett. 245 (2019) 49–52.